

Numerical Simulation Approaches for Phased Array Design

(Invited Paper)

Levent Sevgi

Doğuş University, Electronics and Communication Engineering Department,
Zeamet Sok. No. 21, Acıbadem / Kadıköy, 34722 Istanbul - Turkey

Abstract - This paper reviews the two well-known numerical simulation techniques that are widely used in antenna modeling; the finite-difference time-domain (FDTD) and the Method of Moments (MoM). The packages FDANT (prepared in Fortran language by using FDTD) and NEC2 (public domain code for the MoM) are used to model various types of antenna arrays, their advantages/disadvantages are discussed on characteristic design examples, and they are calibrated one against the other. Also, a simple Matlab package (ANTEN_GUI) for the visualization of radiation patterns, beam forming and beam steering capabilities of user-designed planar arrays of isotropic radiators (which can be used to test the above mentioned packages and as an educational tool, in e.g., antennas and propagation lectures) is introduced¹.

Keywords – Computational electromagnetics, antenna simulation, phased arrays, isotropic radiators, radiation pattern, high frequency radars, ground screen, MATLAB, FDTD, MoM, NEC, three-dimensional graphics, visualization.

I. INTRODUCTION

Recent years have witnessed a lot of research activities focused on the topics of antennas and arrays. For example, smart (intelligent) antennas have started to be used widely to enhance the performance of cellular radio systems. Switched or adaptive beam forming techniques, antenna diversity in combination with enhanced digital signal processing, etc., increase signal quality and channel capacity significantly in comparison with standard antenna configurations. The demand of low cost, small size, but extremely effective smart antennas in both military and commercial Markets make antenna engineers attractive. On the other hand an antenna engineer is required to be more sophisticated, and should be equipped with the theory and practice on a wide range of antennas from basic to state-of-the-art.

An antenna engineer must have strong analytical background and be well-equipped with computer tools and signal processing algorithms. For example, a log-periodic array of monopoles erected over the ground beneath which exist a complicated ground screen design as shown in Fig. 1 requires understanding of high level electromagnetics (EM), ground effects, array design, beam forming, etc. ([1-5] are good examples of classical antenna books), as well as strong numerical computational background together with model validation, software verification and code calibration capabilities.

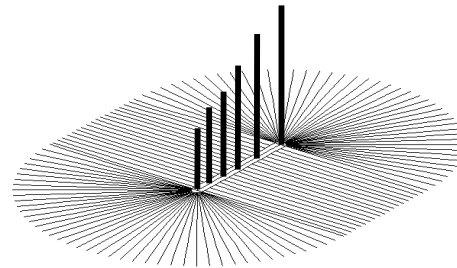


Figure 1. A transmitting antenna array of vertical monopoles for a long-range HF surface wave radar erected above a specially-designed ground screen layout.

One aim of this paper is to review powerful time domain (TD) and frequency domain (FD) numerical antenna simulation tools. Another aim is to supply sample packages, together with the source codes, so that the reader may enjoy running, testing, doing comparisons, as well as developing new modules for the other calculations that are not included in the packages. Although the perspectives of a code developer and a user are quite different the antenna engineer should be well-equipped in terms of both. Since a developer leaves only a small set of tuning parameters that will be supplied by the user, an antenna engineer should develop his/her own codes in order to have maximum flexibility and capability in numerical designs and simulations.

¹ANTEN_GUI, FDANT and their source codes can be downloaded from <http://www3.dogus.edu.tr/lsevgi>

Numerical simulation approaches have long been applied to the design and/or investigation of various types of antennas, from wire arrays to microstrip patches. There are many FD and TD handy simulation tools that are widely used by antenna engineers. The pioneering one is the Numerical Electromagnetic Code (NEC) which is based on the Method of Moments [6] and has many versions. They have been in use for more than a few decades [7]. The public domain simulator NEC2 can easily be downloaded from many internet sites [8], or can easily be purchased with a price less than a few hundred dollars [9] (mostly, the price goes to the supplied graphical user interfaces).

An FDTD based TD simulator FDANT is designed to investigate (although not restricted to) wire antenna arrays of 1D and 2D in free-space and their beam steering capability [10]. FDANT contains almost every major routines, FDTD iterations, PML blocks, NTFP routine, power routines, etc. to direct interested users towards building his/her own antenna simulator, by just adding a specifically designed GUI. The user may also make modifications in source codes of FDANT to simulate other complex antenna structures.

FDTD discretizes Maxwell's equations directly in TD by replacing partial derivatives with their finite difference approximations. Since Maxwell's equations models TD EM wave scattering (i.e., it is an *initial-value problem*) boundary conditions must be satisfied artificially during the simulations. Moreover, since far fields are of interest in order to calculate antenna radiation patterns, this can not be done directly with a *finite-volume* FDTD method; therefore a near-to-far-field (NTFF) transformation is a must in this case. On the other hand, MoM is an FD method and first requires derivation of the Green's function of the problem at hand (i.e., it is a *boundary-value problem*). Then, segmentation is used and a set of equations is formed for the N -segment geometry to calculate surface currents induced by the incident/excitation fields. While the physical size of the problem is critical in FDTD simulations, the most critical parameter in MoM is the number of segments.

II. SIMULATION APPROACHES

Three simulation packages have been outlined in this Section. First, beam forming capability of various planar arrays of isotropic radiators is investigated analytically. A simple, but effective and educating Matlab package – ANTEN_GUI – is introduced [11]. Then the public NEC2 package is reviewed shortly. Finally, the TD FDTD-based simulator FDANT is discussed briefly.

2.1 A Matlab package: Anten_GUI based on analytical formulations

The radiation pattern of a group of isotropic radiators is determined by the type of individual elements, their location, spacing, orientation, excitation amplitudes and phases. In general, the total electric field (which is known as the array factor) of an N -element array located at (x_i, y_i, z_i) ($i=1, \dots, N$) and at a far field point along (θ, ϕ) direction (under $\exp(-j\omega t)$ assumption) is

$$E(\theta, \phi) = \sum_{i=1}^N I_i e^{j\psi_i(\theta, \phi)} \quad (1)$$

where I_i is the complex current for the i^{th} element [12]. The phase contribution ψ_i is at the far field point from the i^{th} radiator with respect to the origin. For the planar arrays located at xz -plane the array factor can be expressed as:

$$E(\theta, \phi) = \sum_{i=1}^N I_i \exp(jkr_i \sin \theta \cos(\phi_i - \phi)) \quad (2)$$

This expression corresponds to the pattern of arbitrarily-located, isotropic, equi-amplitude, non-phased radiators when $I_i = 1.0$. The main beam of an array can be steered electronically by varying the phases of the currents applied to the array elements. Equation 2 takes on the form of

$$E(\theta, \phi) = \sum_{i=1}^N I_i \times \exp\{jkr_i [\sin \theta \cos(\phi_i - \phi) - \sin \theta_0 \cos(\phi_i - \phi_0)]\} \quad (3)$$

if the beam angle is specified as (θ_0, ϕ_0) . This means each element is phased accordingly to direct the beam of the array along (θ_0, ϕ_0) direction. It reduces to (2) when $\theta_0 = 0^\circ$, therefore it represents “no-phasing”. The default θ_0 value is zero in the GUI and should be kept as it is if one does NOT want to phase elements.

Extra line phasing capability can be added to change front-to-back (FBR) characteristics in the planar array option. The user may change the phase angle $\Delta\beta$ of the lined-up radiators and observe how FBR improves or gets worse. In this case complex currents I_i in (3) is replaced with I_{in} as

$$I_i \rightarrow I_{in} = \sum_{n=1}^M I_i \exp\{j(n-1)\Delta\beta\} \quad (4)$$

For an $N \times M$ planar array, if for example, a phase of $\Delta\beta = 30^\circ$ is selected, then the phases of the second row ($M=2$) lag 30° the phases of the first row ($M=1$), the phases of the third row ($M=3$) lag 30° the phases of the

second row ($M=2$), and 60° the phases of the first row ($M=1$), etc.

The Matlab-based antenna package ANTEN_GUI has been prepared for the visualization of radiation characteristics of planar arrays of isotropic radiators (see Fig. 2) [11,12]. The package allows the user to choose different types of arrays with a number of user-selected and located isotropic radiators. The default array type is *arbitrary*. Once the number of radiators (N), maximum radius (in meters) of the polar region where the radiators will be located, and the operating frequency (in MHz) are specified, the user may proceed to locate the radiators one by one after pressing the “Locate Radiators” button. The coordinates of the located radiators are also displayed in the list-box at the bottom.

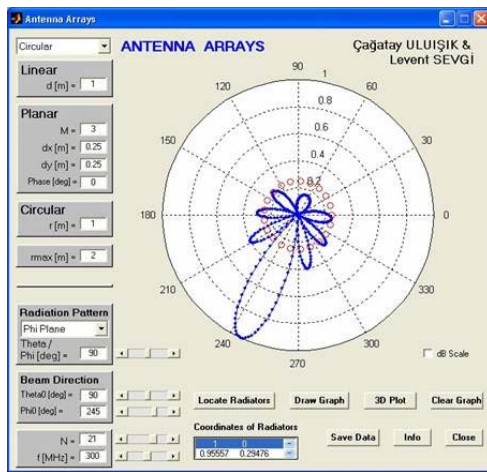


Figure 2. The ANTEN_GUI front panel that shows the radiation pattern of a 21-element circular array located on the xy -plane ($f=300$ MHz, the radius is $r=0.5$ m ($\lambda/2$), elements are phased in a way that the beam points $\theta_0=90^\circ$, $\phi_0=245^\circ$).

By clicking the mouse the user may design any kind of an array, but the package also locates the radiators automatically when one of the other types of the arrays is selected and required parameters are supplied (see Fig. 3). If the array type is set to *linear*, N -elements are located on the y -axis symmetrically, with an inter-element distance of d . If it is planar, $N \times M$ elements are located on xy -plane. In this case, N and M are the number of the elements along y - and x -directions, respectively. The distances between the radiators along x - and y -directions are dx and dy , respectively. If the circular array type is selected, N -elements are located symmetrically on a circle whose center is at the origin and radius is r .

After locating the radiators the user may visualize a 2D radiation pattern at the selected plane by pressing the “Draw Graph” button. The 2D radiation pattern plane to be displayed is specified by the *Theta/Phi Plane* popup menu and *Theta/Phi value* box. If the θ -plane is selected (vertical pattern) the angle θ varies between $[0^\circ, 360^\circ]$ at a fixed ϕ value (specified by the *Theta/Phi* box). If the ϕ -plane is selected, the angle ϕ varies between $[0^\circ, 360^\circ]$ at a fixed θ -value specified by the user; the radiation pattern in this case is called “horizontal”. All the 2D radiation patterns are plotted with an angular resolution of $\Delta\theta=\Delta\phi=1^\circ$.

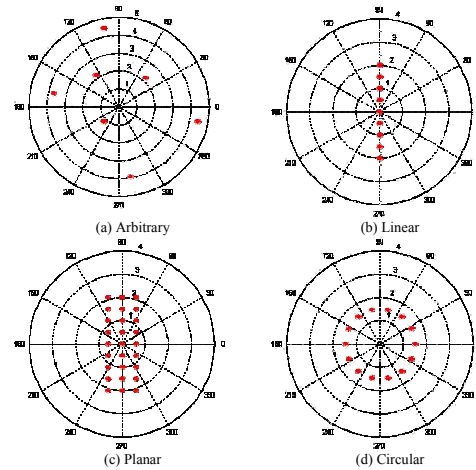


Figure 3. Different geometrical configurations of planar arrays of isotropic radiators that can automatically be located once the number of radiators is chosen, (a) arbitrary, (b) linear, (c) planar, and (d) circular arrays.

Fig. 2 shows the radiation pattern of an arbitrarily-located 7-element array. The user selects the radiation pattern plane and the beam direction from the front panel (on the bottom-left). In this example, the pattern belongs to ϕ -plane (i.e., on the xy -plane) since $\theta=90^\circ$. The beam angles are selected to be $\theta=90^\circ$ and $\phi=245^\circ$. In Fig. 4, horizontal radiation pattern ($\theta=90^\circ$) of a planar array of 5×1 (i.e. a 5-element linear array) is shown as an example. Here, frequency is 300 MHz, beam angles are $\theta_0=90^\circ$ and $\phi_0=90^\circ$, and inter-element distance is 0.4 m (0.4λ).

ANTEN_GUI also has a 3D radiation pattern plotting capability. The approach [13] (in dB scale with a 30 dB margin along each axis) is based on normalization of the radius of the unit sphere for each observation angle (θ_i, ϕ_i) in 3D Cartesian coordinates according to the radiation intensity calculated from (3). The angular resolution for the 3D plots is set to be $\Delta\theta=\Delta\phi=2.5^\circ$

which means the calculations are repeated at $151 \times 151 = 22,801$ vertices.

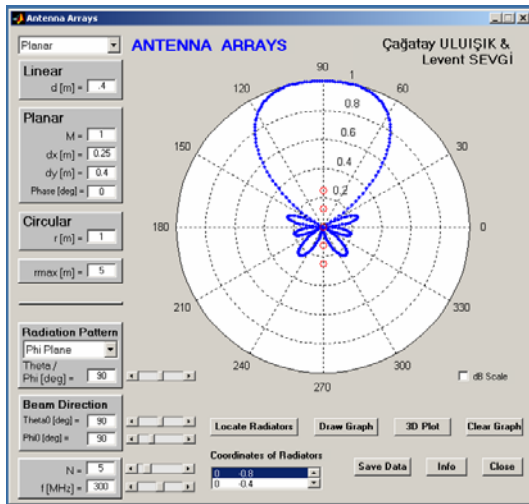


Figure 4. The H-plane (horizontal) 2D radiation pattern of a 5-element linear array ($f=300$ MHz, inter-element distance is $d=0.5$ m ($d=\lambda/2$), beam angles are $\theta_0=90^\circ$ and $\varphi_0=0^\circ$).

The 3D radiation pattern of the array given in Fig. 4 is plotted in Fig. 5 as an example.

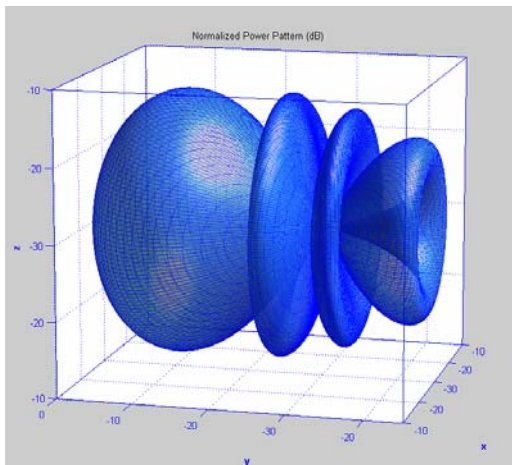


Figure 5. The 3D radiation pattern of the same 5-element linear array ($f=300$ MHz, inter-element distance is $d=0.5$ m ($d=\lambda/2$), beam angles are $\theta_0=90^\circ$ and $\varphi_0=0^\circ$).

Another exciting feature of ANTEEN_GUI is that the user can use sliding bars to change N , f , θ_0 , φ_0 . For instance, by pressing the sliding bar of the frequency continuously, the user can increase or decrease the frequency, see the corresponding radiation pattern

immediately, and may easily understand the effect of frequency change on the radiation pattern. The package also allows the user to save the radiation pattern data (field intensity vs. angle) to a file named *Arraypattern.dat*. The first column of this file corresponds to 361 observation angle values (in radians), and the corresponding array factors are in the second column.

Any 2D array may be designed by the user and its radiation characteristics can be investigated. Beam forming capabilities for different locations, number of radiators, as well as for operating frequencies can be visualized. The package may be used as an educational tool in many undergraduate antenna lectures. It may also be used to validate and verify the FDTD and MoM packages described below. Moreover, the reader may add novel features to the supplied source codes, such as a module for the formation of 3D (volume) arrays which is straightforward.

2.2 NEC2 package based on FD Method of Moments (MoM) technique

The NEC is an outgrowth of a program developed in the 1970s, called the Antenna Modeling Program (AMP). It has been developed at the Lawrence Livermore Laboratory, Livermore, California, under the sponsorship of the Naval Ocean Systems Center and the Air Force Weapons Laboratory [7]. There are at least 4 versions of NEC, with NEC2 emerging in 1981 and NEC4 appearing in 1992. NEC2 is the highest version of the code under public domain. NEC4 remains proprietary with the Lawrence Livermore National Laboratory (as far as the author's knowledge,) and the University of California. It requires a separate license for use.

NEC in all its forms is a computer code for the analysis of the EM response of antennas and other metal structures that uses MoM techniques. It is a numerical solution to integral equations for the currents induced on a metallic structure by sources or incident fields. The approach has no theoretical limit and may be used for very large arrays or for the very fine subdivision of smaller arrays. Any geometry (e.g., a loop antenna, helical antenna, a monopole over a rectangular PEC box, an array over the ground with complex ground screen layout, a radio antenna on a car, a radar antenna beneath an aircraft, etc.) can be modeled with NEC as long as their mesh representation can be built, which is the most difficult (and time-consuming) part in NEC simulations.

It should be noted that all the radiating elements of the antenna structure must be in a volume bounded by the

near-field criteria; otherwise the presented patterns become invalid.

2.3 The FDTD-based antenna simulations and FDANT package

FDTD technique [14] depends on the solution of Maxwell's equations directly in time domain, where the physical geometry is divided into small (mostly rectangular or cubical, but non-orthogonal in general) cells. Both time and spatial partial derivatives are handled with finite- (central-) difference approximation and the solution is obtained with a marching scheme in iterative form. The characteristics of the medium are defined by three parameters; permittivity, conductivity and permeability, and three electric and three magnetic field components are calculated at different locations of each cell.

The FDTD has almost become a standard tool for antenna simulations for the last decade or so (see, e.g., [15-17] for our studies). The addition of powerful absorbing boundary simulators (such as perfectly matched layers, PML), and near-to-far field transformation (NTTF) either in FD or TD, has made it possible to simulate almost any kind of complex structure's radiation characteristics. An example [17] is given in Fig. 6 and the radiation and beam steering capabilities are presented in Fig. 7.

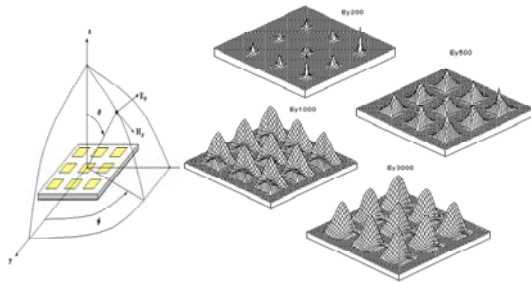


Figure 6. A 3×3 microstrip patch array designed to form a main beam of 35° at 1.8 GHz and near-field transient behaviors at different time instants (FDTD parameters: $\Delta x = \Delta y = 2.758$ mm, $\Delta z = 0.250$ mm, $w = 5.516$ mm $= 20 \times \Delta x$, $h = 1$ mm $= 4 \times \Delta z$, $\epsilon_r = 2.2$, $a = 18 \times \Delta$, $b_y = 5 \times \Delta$, $b_x = 7 \times \Delta$).

In Fig. 6, a 3×3 coax-fed microstrip patch array (which is designed to form a main beam of 35° at 1.8 GHz) is illustrated. Near field values at different time instants calculated inside the FDTD volume are also plotted in the figure. The FDTD parameters of this simulation are as follows: $\Delta x = \Delta y = 2.758$ mm, $\Delta z = 0.250$ mm, $w = 5.516$ mm $= 20 \times \Delta x$, $h = 1$ mm $= 4 \times \Delta z$, $\epsilon_r = 2.2$, $a = 18 \times \Delta$, $b_y = 5 \times \Delta$, $b_x = 7 \times \Delta$. The radiation patterns in Fig. 7 are at 1.8

GHz, left: $\phi = 0^\circ$, right: $\phi = 90^\circ$. The first row corresponds to feeding without time delay (i.e., without phasing in FD). The second row corresponds to feeding with delays of 0.094 ns which points the main beam towards $\theta = \pm 20^\circ$, respectively.

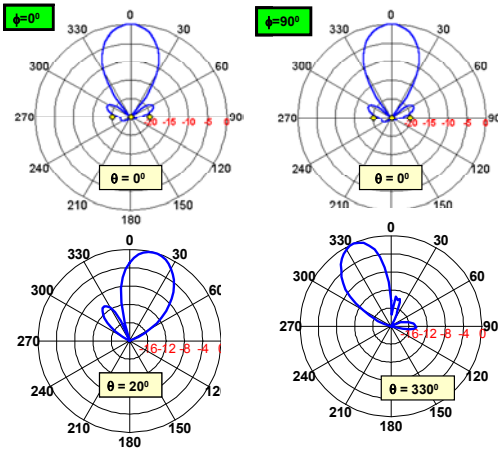


Figure 7. Radiation patterns at 1.8 GHz, left: $\phi = 0^\circ$, right: $\phi = 90^\circ$. First row: feeding without time delay (i.e., without phasing in frequency domain). Second row: feeding with delays of 0.094 ns which points the main beam towards $\theta = \pm 20^\circ$, respectively.

FDANT is supplied in [10] and can be used for antenna analysis. Its structure is given in Fig. 8. It first reads user defined parameters from the input file ANT.INP. Transient analysis is done within FDTD computation space for short-pulse excitations, and TD output data is stored in three different files. SOURCE.dat contains time vs. source amplitude to allow the user to see the excitation signal in TD. AN-NEAR.dat has near field E_z values in two columns; time in [ns] and E_z in [V/m]. Finally, AN-FAR.dat has TD far field data along the number of chosen directions, obtained via NTFF transformation directly in TD.

FDANT is prepared to investigate vertical or horizontal radiation patterns for a 2D array of maximum 2 by 6 elements (but, the size of the array may be changed by the user). The array is located longitudinally along y -direction (see Fig. 9). The elements are half-wavelength, vertical, center-fed dipoles. Inter-element distance along y -direction is " d " and supplied by the user. Inter-element distance along x -direction is automatically set as " $d/2$ ". The lengths of the dipoles are set as " $d/4$ ". The excitation is a short pulse of modulated Gaussian function. The modulation signal and bandwidth is determined automatically to include frequencies for the first few resonances. The user may decide which row to excite; both, front row or back

row. These are all given by the user in the input file ANT.INP explained in Table 1.

Table 1. The ANT.INP and required parameters.

Row	Parameter
1	# of elements in X [1-2], # of elements in Y [1-6]
2	Inter-element distance along Y [m]
3	Excitation (0: Both rows, 1: Front Row, 2: Back Row)
4	Delay [sec]
5	Observation point for near fields (Obsx, Obsy, Obsz)
6	Pattern Plane [1-0] (1: Vertical Pattern, 2: Horizontal Pattern)
7	Angle [deg] PHI (for Vertical Pattern), Theta (for Horizontal Pattern)

In ANT.INP file, fourth line is reserved for time delay to allow the antenna array to steer its beam in azimuth. The calculation of this delay for an array to steer ϕ degrees from antenna bore-sight (from x-direction) is given in Fig. 9. Since the array is in free-space velocity of light (c) and inter-element distance (d) are used to calculate the delay (τ). This is the delay of the second element with respect to the first one. The third, fourth, etc. elements have delays of " 2τ ", " 3τ ", etc., respectively.

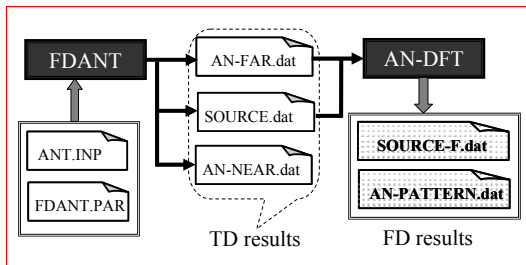


Figure 8. The flow chart of the FDTD-based antenna simulator FDANT. The package calculates radiation patterns of a given array by using broadband (pulse) excitation, near-field EM simulation inside the FDTD volume terminated by powerful perfectly matched layer (PML) blocks, near-to-far-field transformation directly in time domain, and finally by applying off-line DFT all around on a chosen radiation plane.

When the simulation is run, it first requires selection of (vertical or horizontal plane) radiation pattern. Then, angular resolution is supplied. If for example, horizontal plane radiation pattern is selected with 2° resolution, NTF transformation is applied at 181 assumed directions (with 2° angular separation) inside the TD loop (although they are same, calculations at 0° and 360° are performed separately, only for graphical

illustrations). The results are written to the output file AN-FAR.DAT. There are four columns in this file: These are the angle, time, E_θ and E_ϕ . If the number of time steps and angle are NSTOP and 181, respectively, then the number of lines will be NSTOP+200 for each angle with a total of $181 \times (NSTOP+200)$.

It should be noted that, extrapolated TD far fields are stored in a time array, and dimension of this array must be greater than the number of simulation time steps, NSTOP. This is due to TD far field extrapolation as explained in [10]. Here, 100 time cells are reserved for this transformation in front, and at the back of the array. This is why the total simulation time will be NSTOP+200.

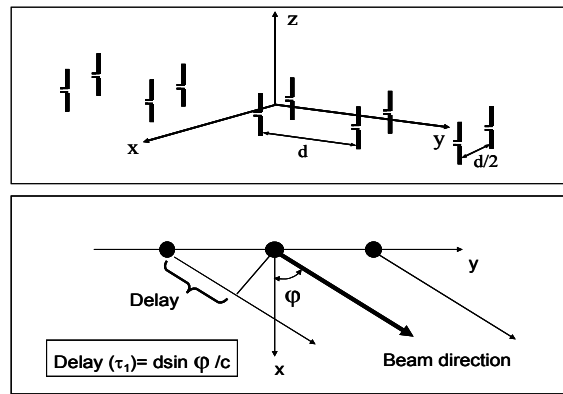


Figure 9. The location and parameters of the 2×5 of vertical, center-fed wire array; inter-element distance (along x-direction) is $d/2$, but inter-array distance (along y-direction) is d . The beam direction and the excitation delay to obtain this direction is also shown.

The user may select to use a short pulse or a single frequency sinusoidal excitation in TD simulations. Choosing a short-pulse, results in a broad band response with a single TD run. FDTD based simulation yields broad band response in time domain. Radiation patterns at multiple frequencies are computed by the Fortran program AN_DFT (it should be noted that source codes FDANT.FOR, FDANT.PAR and AN-DFT.FOR are also included, therefore any user who is familiar with the classical FDTD method can directly go into the codes and do the analysis of their own structures).

III. DESIGN EXAMPLES

Characteristic antenna structures are presented in this Section to discuss capabilities of the FDANT and NEC2 packages. Since FDANT uses 3D FDTD volume and NTF transformation routine any kind of antenna structure can be simulated with this package. The only restriction is the computer memory and the speed,

therefore the larger the structure (or the higher the number of elements in the array) the higher the requirement for large memory and high-speed. With today's regular PC (e.g., with 1 GB RAM Memory) a cubical volume of $250 \times 250 \times 250$ (nearly 20 million cell volume) (i.e., $25\lambda \times 25\lambda \times 25\lambda$ volume with $\lambda/10$ rough discretization at the highest frequency) can be handled in a few minutes (with a 4-GHz-CPU speed).

NEC2 uses the coordinates of the antennas in 3D Cartesian coordinate system and represents wires with small pieces called *segments* (roughly with maximum segment lengths of $\lambda/10$). Any length of an array may be located as long as long as the number of segments is less than the number that can be handled via the PC at hand (e.g., less than ten thousand segments). An N -segment system is represented a linear system of equations with N -unknowns (i.e., segment currents) and N -equations. The MoM is a semi-analytical method which requires the Green's function of the problem at hand [6].

One should be aware of the assumptions and approximations made in and the limitations of the packages at hand. FDANT is based on discretization of 4D Maxwell's equations from very beginning; therefore it may be accepted as a reference solution (as long as parameters are chosen accordingly). On the other hand, NEC2 does not take the diffraction (secondary) effects into account.

Finally it should be remembered that FDANT simulates near EM transient fields in TD and then gives the radiation patterns in FD via the application of off-line DFT. NEC2 simulates far field interference effects of elements along a chosen direction in FD and yields the radiation pattern. Although time-consuming multi-frequency responses can be obtained via a single FDANT simulation, while NEC2 requires repeat ion of the calculations for every frequency.

3.1 Wire and loop (resonant) arrays (FDANT vs. NEC2)

Arrays of wire antennas in free-space are basic structures that can easily be handled via both FDANT and NEC2 packages. Two typical comparisons between FDANT and NEC2 are given in Figs. 10 and 11.

Very good agreement between results of the two methods is clearly seen in the plots. This should be expected because the structures are rectangular and contain no curvature, therefore discretization error is minimal. Note that the array can not steer beams beyond $\varphi = \pm 45^\circ$ as clearly observed in the figures. The beams formed in these figures are forward/backward

symmetric with zero FBR. To direct energy forward the two corresponding elements in x-direction must be an end-fire property. At 250 MHz (i.e., inter-element distance along x is $\lambda/4$ and inter-array distance along y is $\lambda/2$) this may be satisfied by giving extra delay of $d/2c$ in FDANT (90° phase lag in NEC2). Fig. 12 shows the horizontal patterns for this scenario.

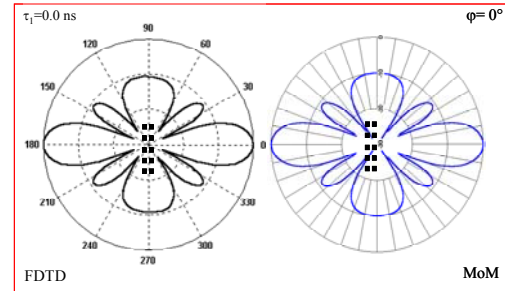


Figure 10. A sample radiation pattern of the 2×5 array on the xy -plane ($f=250$ MHz, $d=\lambda/2$, $\tau_1=0$ s, $\theta=90^\circ$, $\varphi=0^\circ$), left: FDTD, right: MoM (NEC2).

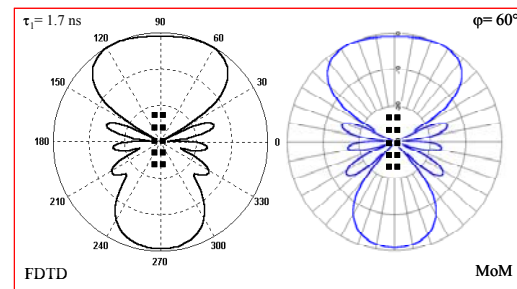


Figure 11. A sample radiation pattern of the 2×5 array on the xy -plane ($f=250$ MHz, $d=\lambda/2$, $\tau_1=1.7$ s, $\theta=90^\circ$, $\varphi=60^\circ$), left: FDTD, right: MoM (NEC2).

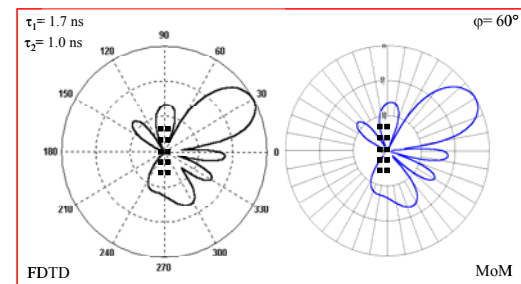


Figure 12. A sample radiation pattern of the 2×5 array on the xy -plane ($f=250$ MHz, $d=\lambda/2$, $\tau_1=1.7$ s, $\tau_2=1.0$ s, $\theta=90^\circ$, $\varphi=60^\circ$, 90° between the first and second rows), left: FDTD, right: MoM (NEC2).

Another structure used in FDANT and NEC2

comparisons is a 2×10 square loop array. Loop antennas form another antenna type, which features simplicity, low cost and versatility. In Fig. 13, the array is given. Each square loop is 0.25 m^2 . By using 4 wires, 40 segments for each square loop, the array is modeled with a total of 800 segments in NEC simulator. With the same discretization ($\Delta x = \Delta y = \Delta z = 2.5 \text{ cm}$) the array needs an FDTD space of $50 \times 230 \times 50$. At 300 MHz, the array correspond to loops with $\lambda/4$ sides and $\lambda/2$ inter-element separation. The simulated radiation patterns and steered beams obtained via both NEC and FDTD simulators are also given in the figure, where vertical field components are plotted.

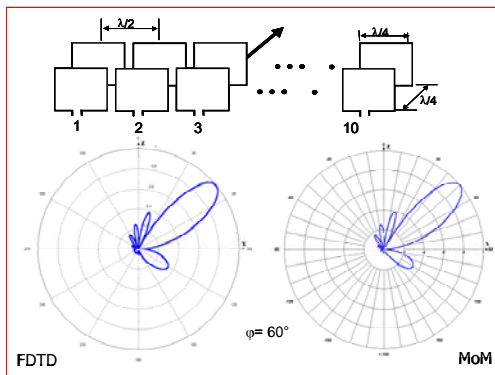


Figure 13. Another sample array of 2×10 rectangular wire antennas on the yz -plane ($f=250 \text{ MHz}$, $d=\lambda/2$, $\tau_1=1.7 \text{ s}$, $\theta=90^\circ$, $\varphi=40^\circ$), left: FDTD, right: MoM (NEC2).

3.2 HFSWR arrays (NEC2)

High frequency surface wave radars (HFSWR) have become attractive systems for wide area (up to 500 km in range and 120° in azimuth) all-weather, continuous surveillance. HFSWR receive array is one typical example that belongs to large-system, complicated arrays. The array must be located near the sea, parallel to the shore line, have high and equal array gain over the entire surveillance area with minimum sensitivity to signals arriving from other directions (especially from ionosphere). Operating at the lower end of the HF band requires that the receive array occupies a significant shoreline area, with the aperture of the array inversely proportional to frequency. For example, at 3 MHz, a 5° azimuth beamwidth requires an array aperture of approximately 800 m - 1 km. Moreover, the receive array should direct its power towards the ocean surface, with high FBR, so that it neither interfere land based other systems, nor is interfered by them. To satisfy all these requirements first elements (i.e., channels) of the array shall be designed to

- form a maximum radiation along the channel axis with as much azimuth coverage as possible (typically $100^\circ - 120^\circ$),
- give as high gain as possible (at least 2-3 dB)
- give as much FBR ratio as possible (at least 12-15 dB),
- give as deep over-head null as possible (at least 25-30dB).

To satisfy these requirements, three different structures (i.e., *quadlet*, *triplet* and *doublet*) are investigated as array channels [18]. In quadlet, four elements are spaced approximately quarter-wavelength apart and are phased to form an end-fire channel. Similarly, three and two elements are used in triplets and doublets, respectively. A short monopole is used as a channel radiator and a 16-radial ground screen layout is used underneath. Fig. 14 pictures the top view of the designs of these channels, where radials of different elements in a channel are connected to each other when intersect.

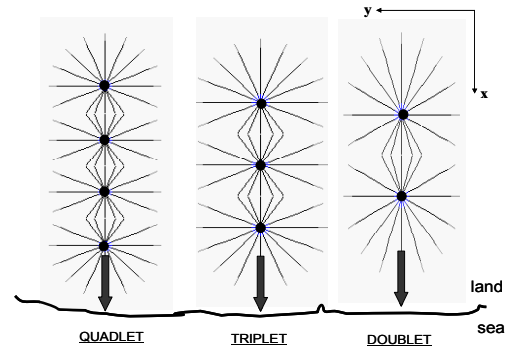


Figure 14. Top view of three different array elements of the HFSWR receiver; doublet, triplet and quadlet, located on the shore of the site, looking towards the sea. The array elements should satisfy high FBR. A ground screen (of 16-element radials) lowers the ground losses.

The channels are optimized for the frequency band of 3 MHz - 6 MHz. The parameters of the channels are listed in Table 2. Ground is assumed to be POOR ($\sigma_g=0.003 \text{ S/m}$ and $\epsilon_g=4.0$). Parameters for the ocean are assumed to be $\epsilon_r=80.0$, $\sigma=5.0 \text{ S/m}$ in NEC calculations, where EM shooting towards ocean surface is simulated. The difference between erecting the antennas over POOR ground or PEC surface may result in a reduction of gain by up to 15 dB. Beside this loss, there is also an extra near field propagation path loss because of the POOR ground.

Table 3 lists vertical electrical field strength and path loss at 1 km away from a 1 kW vertical radiator. It is

clear that, at 1 km distance; propagation loss over POOR ground may be 10-15 dB higher than the propagation loss over ocean surface. Therefore, together with the reduction in antenna gain, there may be a total of 30 dB extra loss just because the antenna elements are erected over POOR ground. A typical solution to overcome this problem is to use ground screen [19].

Table 2. HFSWR Receive array channel parameters.

Parameter	Value
Antenna height	9.22 [m]
Element spacing	19.0 [m]
Element wire radius	0.15 [m]
Number of radials	16
Radial wire lengths	19.0 [m]
Radial wire radius	0.001 [m]
Incremental increase in cable length	19.0 [m]
Phase velocity in electrical cable	$0.84 \times c$ [m/s]

Table 3. Field strength and path loss values of a vertical radiator with 1 kW transmitter power at 1 km distance ($d=1$ km, $\epsilon_g=15.0$, $f=3$ MHz).

Conductivity [S/m]	Field Strength [dB μ V/m]	Path Loss [dB]
0.0001	95.2	56.3
0.001	96.6	55.0
0.01	106.4	45.1
0.1	109.3	42.2
1.0	109.5	42.0
5.0	109.5	42.0

The channel elements discussed here are all bottom fed. The feeder cable losses are represented by voltage drops. The loss of the cable is given as 0.55 dB/100 ft at 10 MHz, therefore 0.5 dB/100 ft cable loss is taken into account within the band of 3 MHz - 6 MHz. For 19.0 m cable length voltage drop corresponds to 5 V. Therefore, elemental feeding voltages are taken as:

Quadlet: 100 V, 95 V, 90 V and 85 V
Triplet: 100 V, 95 V and 90 V
Doublet: 100 V and 95 V.

Vertical and horizontal radiation patterns obtained via NEC2 simulations are given in Figs. 15 and 16. Here, the channels are located along x-axis. Vertical radiation patterns in Fig. 15 are obtained at xz-plane ($\varphi=0^\circ$, $-90^\circ < \theta < 90^\circ$).

On top comparisons of the three proposed channels is given at 4.5 MHz, at the bottom vertical patterns of the quadlet with and without ground screen (16-radial design) at 3.5 MHz. As shown in the figure almost 12-

13 dB improvement is obtained in the channel gain when radials are used. However, employment of a ground screen can be seen to have had a negative effect on direct overhead nulling. The surface-wave coupling effect (for the array 50 m away from the shore line) is also plotted (see the dotted line).

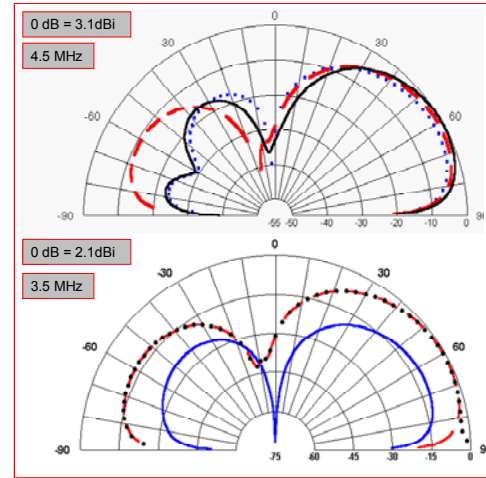


Figure 15. NEC2 simulated vertical radiation patterns of the array elements shown in Fig. 14; (Top) comparisons among the channels ($f=4.5$ MHz, $\varphi=0^\circ$, 0 dB corresponds to 3.1 dBi). Dots: doublet, Dashed: triplet, Solid: quadlet. (Bottom) quadlet with and without radials, solid: without radials, dashed: with radials, dots: surface-wave coupling at 50 m away from the shore line ($f=3.5$ MHz, $\varphi=0^\circ$, 0 dB corresponds to 2.1 dBi). More than 30 dB overhead null is satisfied.

Horizontal radiation patterns in Fig. 16, comparing the three proposed channels at left, and the quadlet with and without radials at right) are plotted 5° above xy-plane ($\theta=85^\circ$, $0^\circ < \varphi < 360^\circ$). As observed in Figs. 15 and 16, quadlet, triplet and doublet as receive array channel elements have similar channel gain and FBR at this frequency. On the other hand, vertical and horizontal back lobe shapes and overhead nulling effects are quite different.

One HFSWR receive array is designed as a 24-channel array by using quadlets [18]. Inter-channel distances are taken as 31 m. With these parameters, a rectangular area of $57 \text{ m} \times 713 \text{ m}$ is required only for the 4×24 monopoles. With ground screen and a security fence this area may be as large as $100 \text{ m} \times 1000 \text{ m}$. The connections between channels are done via underground cables and their lengths are very important since they introduce signal attenuation and phase distortion. Horizontal radiation patterns and electronic beam forming are simulated and illustrated in Fig. 17

for different beam pointing angles. Here, patterns with beam angles 0° , 15° , 55° towards right and -15° , -30° and -60° towards left are plotted. As observed in the figure, for the 0° beam the array has nearly 5° beam width, 30 dB FBR and more than 20 dB side lobe suppression. These performance parameters are almost satisfied for the beams within $\pm 45^\circ$. Acceptable values are obtained when the beam is within $\pm 45^\circ$. On the other hand, unwanted strong side lobes appear when the beam angle is higher than $\pm 45^\circ$ (see the 55° and -60° beams in the figure).

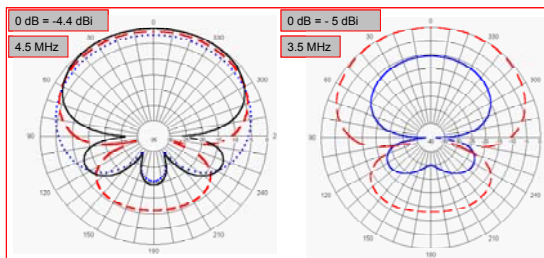


Figure 16. NEC2 simulated horizontal radiation patterns of the array elements shown in Fig. 14; (left) comparisons among the three channels ($f = 4.5$ MHz, $\theta=90^\circ$, 0 dB corresponds to -4.4 dBi). Dots: doublet, Dashed: triplet, Solid: quadlet, (right) quadlet with and without ground screen layout, solid: without radials, dashed: with radials ($f= 3.5$ MHz, $\theta=90^\circ$, 0 dB corresponds to -5 dBi). The front beam characteristics of the array elements do not change significantly.

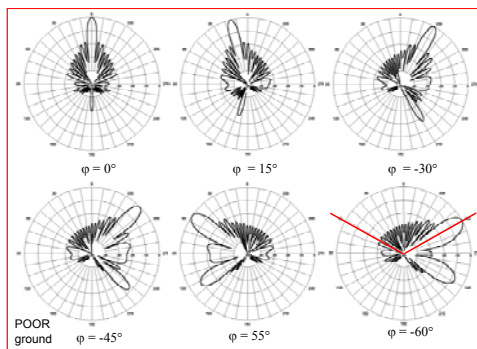


Figure 17. NEC2 simulated horizontal radiation patterns of the 4×24 element monopole array designed for the HFSWR receiver with beam steering capabilities ($f= 3.5$ MHz, $\theta=90^\circ$).

HFSWR is an all-whether, continuous system, and very often one or more channels fail to operate. The operator should know what happens when one or more channels are not working properly. This is simulated in NEC2 and typical results are plotted in Fig. 18. In the 24-channel array, the channels are numbered 1 to 24 from

left to right. The blanked channels are (left) 7-9-10, (right) 11-12-13 in the figure. The thin and thick lines correspond to 24-channel beam forming with and without blanked channels, respectively.

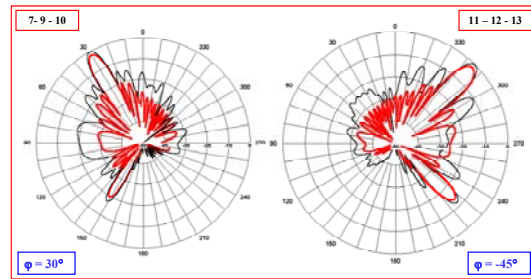


Figure 18. NEC2 simulated channel failure effects of the 4×24 element monopole array designed for the HFSWR receiver ($f= 3.5$ MHz, $\theta=90^\circ$). The top numbers represent the failed channels.

It should be noted that NEC2 does not model diffraction; thus attention must be paid in interpreting its numerical results. Differences above 30 – 35 dB may be practically meaningless because of the diffraction. The example presented in this subsection may also be simulated via the FDTD simulator, but it requires an NTF transformation module for a two-layer volume (the one supplied in FDANT is designed for free-space).

IV. CONCLUSIONS AND DISCUSSIONS

Three different packages are reviewed in this paper. A simple user-friendly antenna array package ANTEN_GUI prepared with Matlab 6.5, the well-known, public domain NEC2 package, and the FDTD-based FDANT package are presented together with some practical array examples that illustrate their capabilities and inefficiencies. Characteristic designs are also given for mutual comparisons.

Roughly speaking, a few tens of millions of cells may be simulated in FDTD in the order of minutes (much less than an hour) with today's regular PC (e.g., 512 MB RAM 1-2 GHz CPU speed), and most of the time is used for NTF process (there is at least an order of magnitude difference between the FDTD simulation and NTF transformation). MoM-based calculations may also be performed in the same PC with similar computation time if the number of segments is less than 2300-2500. Some other critical parameters and comparisons are given in Table 4.

It should be noted that there are highly impressive commercial antenna packages that have been widely used in industry, which may be listed through a quick

internet search. Although it is very handy to use these packages as antenna engineers for design purposes, people should never forget to practice with their own codes if they do research. It may be claimed that practicing with in-house prepared codes first shall also increase performances while using commercial codes.

Table 4. Performance comparisons; FDTD vs. NEC

EVALUATION PARAMETER	FDAND (FDTD)	NEC2 (MoM)
Full wave solution	Accounts for major wave phenomena	Diffraction effects can not be handled
Analytical derivation	Not required	Requires derivation of Green's function
Critical parameter	Cell size & time step (discretization)	Segment in terms of wavelength
Assumptions	Everything is constant inside a cell	Current is constant along the segment
Capability	Broad class of EM problems (antennas, propagation, RCS, EMC, EMI, etc.)	Certain class of antenna and RCS problems
Stability	May be unstable (iterative open-form representation)	Always stable (closed-form representation)
Convergence	Not a problem (as long as stability condition is satisfied)	May be a problem (depending on segmentation)
Computation time	Increases parallel to the # cells	Increases parallel to the # segments
RAM Memory	Huge; increases parallel to the # of cells	Medium; increases parallel to the # segments)
Problem structure	Good for every kind of media	Good for only metallic structures
Geometry error	Should fit into the coordinate system	No restriction (but elements must be inside the coupling region)
Broadband evaluation	Can be obtained with a single-run	Indirectly, requires multi-runs
Beam forming / steering	Controlled via time delay in excitation	Controlled via element phasing

REFERENCES

- [1] E. Jordan and K. G. Balmain, *Electromagnetic Waves and Radiating Systems*, Prentice-Hall, Englewood Cliffs, NJ 1950.
- [2] J. D. Kraus, *Antennas*, 2nd Ed., MacGraw-Hill Book Co., NY 1988.
- [3] C. A. Balanis, *Antenna Theory - Analysis & Design*, 2nd Ed., John Wiley and Sons, Inc., NY 1997.
- [4] R. E. Collins, *Antennas and Radiowave Propagation*, MacGraw-Hill Book Co., NY 1985.
- [5] W. L. Stutzman and G. A. Thiele, *Antenna Theory and Design*, 2nd Ed., John Wiley and Sons, Inc., NY 1998.
- [6] R. F. Harrington, *Field Computation by Moment Methods*, New York, The Macmillan Co., 1968.
- [7] G. J. Burke and A. J. Poggio, "Numerical Electromagnetic Code-Method of Moments, Part I: Program Description, Theory," Technical Document, 116, Naval Electronics System Command (ELEX 3041), July 1977.
- [8] Visit <http://members.home.net/nec2/> and <http://www.emlib.jpl.nasa.gov>.
- [9] Visit <http://www.nittany-scientific.com> or <http://www.poynting.co.za>.
- [10] L. Sevgi, *Complex Electromagnetic Problems and Numerical Simulation Approaches*, IEEE Press – John Wiley and Sons, NY 2003.
- [11] L. Sevgi and Ç. Uluişik, "A Matlab-based Visualization Package for Planar Arrays of Isotropic Radiators," *IEEE Antennas and Propagation Magazine*, Feb 2005.
- [12] B. R. Mahafza and A. Z. Elsherbeni, *MATLAB Simulations for Radar Systems Design*, Chapman and Hall/CRC Press, 2003.
- [13] J. C. Bregains, F. Ares, and E. Moreno, "Visualizing the 3D Polar Power Patterns and Excitations of Planar Arrays with MATLAB," *IEEE Antennas and Propagation Magazine*, Vol.46, No.2, pp.108–112, Apr 2004.
- [14] K. S. Yee, "Numerical solution of initial boundary value problems involving Maxwell's equations," *IEEE Transactions on Antennas and Propagat*, Vol.14, No.3, pp.302-307, May 1966.
- [15] L. Sevgi and S. Paker, "FDTD Based RCS Calculations and Antenna Simulations," *AEU, International J. of Electronics and Commun.*, Vol.52, No.2, pp.65-75, Mar 1998.
- [16] L. Sevgi, "HF Wire Antenna Array Design via FDTD and MoM Techniques," *IEEE Canadian Conference on Electrical and Computer Engineering*, May 9-12, 1999, Alberta, Canada.
- [17] G. Cakir and L. Sevgi, "Design, simulation and test of a low-cost microstrip patch antenna arrays for the wireless communication," Special issue of

ELEKTRİK, Turkish J. of Electrical Engineering and Computer Sciences, Vol. 13, No.1, pp.93-104, 2005.

- [18] L. Sevgi, A. M. Ponsford, and H.C. Chan, "An Integrated Maritime Surveillance System Based on Surface Wave HF Radars, Part I – Theoretical Background and Numerical Simulations," *IEEE Antennas and Propagation Magazine*, Vol.43, No. 4, pp. 28-43, Aug 2001.
- [19] A. M. Ponsford, L. Sevgi, and H.C. Chan, "An Integrated Maritime Surveillance System Based on Surface Wave HF Radars, Part II – Operational Status and System Performance," *IEEE Antennas and Propagation Magazine*, Vol.43., No.5, pp.52-63, Oct 2001.



Levent Sevgi was born in Akhisar, Turkey in 1958. He received his B.S., M.S. and Ph.D. degrees in EE from Istanbul Technical University (ITU) in 1982, 1984 and 1990, respectively. In 1987, he was awarded a fellowship that allowed him to work with Prof. L. B. Felsen at Weber Research Institute/New York Polytechnic University York for two years. His work at the Polytechnic concerned the propagation phenomena in non-homogeneous open and closed waveguides. He became assistant (ITU), associate (ITU) and full professor (Doğuş University) in 1991, 1996 and 2002, respectively.

He was with the Center for Defense Studies, ITUV-SAM for the Long Horizon Project – Integrated Maritime Surveillance System – studies of the Turkish Navy during 1993-1997. He was with the Scientific Research Group of Raytheon Systems Canada from Sep 1998 till Jun 1999 for surface wave HF Radar based Integrated Maritime Surveillance System trials. By invitation, he joined TUBITAK-MRC, Information Technologies Research Institute as the Chair of Electronic Systems Department and spent two years from Jun 1999 till Aug 2000. He was also with ITUV-SAM for Vessel Traffic System installation for Turkish Straits during 2000 - 2002. Since Feb 2002, he has been with ECE Department of Engineering Faculty of Doğuş University in Istanbul.

His research study has focused on propagation in complex environments, analytical and numerical methods in electromagnetics, EMC/EMI modeling and measurement, radar systems, surface wave HF radars, radar cross section modeling and bio-electromagnetics. He is a senior member of IEEE and a member of Turkish Chamber of Electrical Engineers (EMO).

He is the author or co-author of more than 100 journal and international conference papers, 6 books (1 in English, 5 in Turkish), and 2 book chapter.